


Article

Holocene Paleoclimate Changes around Qinghai Lake in the Northeastern Qinghai-Tibet Plateau: Insights from Isotope Geochemistry of Aeolian Sediment

Qiang Peng^{1,2}, Chongyi E^{1,2,3,*}, Xiangzhong Li^{3,4}, Yongjuan Sun^{1,2,3}, Jing Zhang^{1,2,3}, Shuaiqi Zhang^{1,2}, Yunkun Shi^{1,2}, Xianba Ji^{1,2} and Zhaokang Zhang^{1,2}

- ¹ Qinghai Provincial Key Laboratory of Physical Geography and Environmental Process, College of Geographical Sciences, Qinghai Normal University, Xining 810008, China; pqiang0503@163.com (Q.P.); yongjuansun@163.com (Y.S.); 14789911127@163.com (J.Z.); zshuaiqi@126.com (S.Z.); shiyunkun1995@foxmail.com (Y.S.); xianbaji2021@163.com (X.J.); zzk199818@163.com (Z.Z.)
- ² Key Laboratory of Tibetan Plateau Land Surface Processes and Ecological Conservation (Ministry of Education), Qinghai Normal University, Xining 810008, China
- ³ Academy of Plateau Science and Sustainability, People's Government of Qinghai Province and Beijing Normal University, Xining 810008, China; xzhl04@163.com
- ⁴ Yunnan Key Laboratory of Earth System Science, Yunnan University, Kunming 650500, China
- * Correspondence: echongyi@qhnu.edu.cn

Abstract: The stable carbon isotope composition of total organic matter ($\delta^{13}\text{C}_{\text{org}}$) has been utilized in aeolian sediments, serving as an indicator for reconstructing terrestrial paleoenvironments. The Qinghai Lake (QHL) Basin is a climate-sensitive region of significant importance in paleoclimatic reconstruction. However, the reconstructed climatic variations based on $\delta^{13}\text{C}_{\text{org}}$ in aeolian sediments in the QHL Basin in the northeastern Qinghai-Tibet Plateau (QTP) are lacking, and their paleoclimatic significance remains poorly understood. By conducting $\delta^{13}\text{C}_{\text{org}}$ measurements on the Niaodao (ND) aeolian profile near QHL, we reconstructed the paleoclimate changes of 11 ka–present. The variation range of the $\delta^{13}\text{C}_{\text{org}}$ values in the ND profile indicated the terrestrial ecosystems were not the sole contributor to lacustrine organic matter. The $\delta^{13}\text{C}_{\text{org}}$ values are an indicator of historical temperature changes in the study area, exhibiting similar trends with the reconstruction of Chinese summer temperatures, East Asian air temperature, global temperature, and Northern Hemisphere summer insolation at 37° N. The temperature increased with high frequency and amplitude oscillations, with strong aeolian activity and low total organic carbon accumulation during the Early Holocene. The temperature was maintained at a high and stable level, with the weakest aeolian activity and intensified pedogenesis during the Middle Holocene. The temperature decreased at a high rate, with renewed aeolian activity and weak pedogenesis during the Late Holocene.

Keywords: Holocene; soil $\delta^{13}\text{C}_{\text{org}}$; aeolian sediment; total organic carbon (TOC); paleoclimate; Qinghai Lake



Citation: Peng, Q.; E, C.; Li, X.; Sun, Y.; Zhang, J.; Zhang, S.; Shi, Y.; Ji, X.; Zhang, Z. Holocene Paleoclimate Changes around Qinghai Lake in the Northeastern Qinghai-Tibet Plateau: Insights from Isotope Geochemistry of Aeolian Sediment. *Atmosphere* **2024**, *15*, 833. <https://doi.org/10.3390/atmos15070833>

Academic Editor: Wei-Ping Hu

Received: 21 April 2024

Revised: 4 July 2024

Accepted: 11 July 2024

Published: 12 July 2024



Copyright: © 2024 by the authors. Licensee MDPI, Basel, Switzerland. This article is an open access article distributed under the terms and conditions of the Creative Commons Attribution (CC BY) license (<https://creativecommons.org/licenses/by/4.0/>).

1. Introduction

The Qinghai-Tibet Plateau (QTP) is situated at a climatic crossroads where the westerly system, Indian Summer Monsoon (ISM), and East Asian Summer Monsoon (EASM) strongly interact. The Qinghai Lake (QHL) Basin is located in the northeastern part of the QTP and is one of the most climate-sensitive regions on the plateau. This is of significant importance for paleoclimatic reconstruction [1]. Lacustrine sediments are important carriers for climate reconstruction. A spectrum of environmental and climatological reconstructions has been executed in the QHL, predicated on a diversity of climatological proxies [2–7]. Numerous studies have employed a variety of biogeochemical examinations of QHL sediments to reconstruct the regional environmental evolution [2,4,8]. However, there researchers disagree on the interpretation of their environmental significance. The

stable carbon isotope composition of total organic matter ($\delta^{13}\text{C}_{\text{org}}$) is frequently used to trace paleoenvironmental changes in lakes [4,9]. This research suggests a gradual trend from the warm and wet Early Holocene to the cool and dry Late Holocene. High-resolution and continuous climatic records were obtained from lacustrine sediments. However, radiocarbon dating of sediment cores from the QHL faces challenges owing to the lake reservoir effect [10,11]. This refers to the discrepancy between the calendar age and that of the organisms or materials found within the lake sediment owing to the mixing of water with varying residence times and the incorporation of older carbon from the catchment area [11,12]. Additionally, conflicting proxies within lacustrine sediments contribute to the controversy regarding the Holocene climatic fluctuations observed in the QHL [1,2,10,11]. The climate of the QHL area has been suggested to have been dry in the Middle Holocene, compared with the wettest Early Holocene, as inferred from carbonate and ostracod shell $\delta^{18}\text{O}$ values [1]. However, based on pollen assemblage and redness, other studies have suggested a wet climate in the Middle Holocene from the Early Holocene [2].

$\delta^{13}\text{C}_{\text{org}}$ has been widely used in terrestrial sediment as a significant indicator for reconstructing the terrestrial paleoenvironment worldwide [13–16]. In the peat bogs of the QHL Basin, plant $\delta^{13}\text{C}_{\text{org}}$ is regarded as a crucial indicator of summer precipitation. $\delta^{13}\text{C}_{\text{org}}$ is used to trace precipitation variation in the study area in the past 8.4 ka [17]. Holocene aeolian profiles are widely distributed throughout this region [18]. Several studies have been conducted on the $\delta^{13}\text{C}_{\text{org}}$ in aeolian sediments from the QHL Basin and infer that the organic constituents present in the QHL sediments during the Holocene were predominantly derived from the aquatic biota inhabiting the lake [19]. However, owing to the low deposition rate and discontinuity in aeolian sediment, the systematic reconstructed climatic variations based on $\delta^{13}\text{C}_{\text{org}}$ in aeolian sediments in the QHL Basin remain lacking. In this study, the Niaodao (ND) aeolian sediment profile, with a high resolution and continuity on millennium scales [20], around QHL was selected to analyze the variation of the $\delta^{13}\text{C}_{\text{org}}$ and total organic carbon (TOC). There is increasing evidence that temperature has played a crucial role in influencing the soil $\delta^{13}\text{C}_{\text{org}}$ during the Holocene [16,21]. This opens up the possibility of using the $\delta^{13}\text{C}_{\text{org}}$ indicator to quantify Holocene temperatures [21,22]. The $\delta^{13}\text{C}_{\text{org}}$ of the ND profile was used as a proxy of temperature change. In conjunction with the high-resolution chronological framework, TOC, low-frequency magnetic susceptibility (χ_{lf}), and median grain size (Mz), environmental records on the QHL Basin were reconstructed to further understand climate change on the northeastern QTP during the Holocene. This study further extends the applicability of the $\delta^{13}\text{C}_{\text{org}}$ indicator in paleoclimate reconstruction.

2. Materials and Methods

2.1. Study Area

QHL (36.53–37.25° N, 99.61–100.78° E, 3198 m), nestled in the northeastern region of the QTP, holds the distinction of being the largest inland lake in China. Early to Middle Pleistocene lakes began to form in the Qinghai Basin as tectonism topographically separated it from the Yellow River drainage [18]. As of 2019, the water surface area of the QHL had reached 45,190.2 km² [23] (Figure 1). The climate in the QHL Basin is influenced by both the Asian monsoon (EASM and ISM) and westerly system (Figure 1). The winters are dry and cold, whereas the summers are wet and warm. The temperature in this area varies significantly with altitude, with an annual average temperature ranging from −4.5 to 4.0 °C. The average annual precipitation is 350–450 mm, with a decreasing trend from southeast to northwest [24]. The Gangcha meteorological station, positioned 10 km north of QHL, recorded a total precipitation of 370 mm and an average temperature of −0.6 °C between 1975 and 2011. The maximum wind speed, registered at 18 m s^{−1}, predominantly occurs during spring [20]. The predominant vegetation types in the region are temperate steppes, deserts, and alpine meadows.

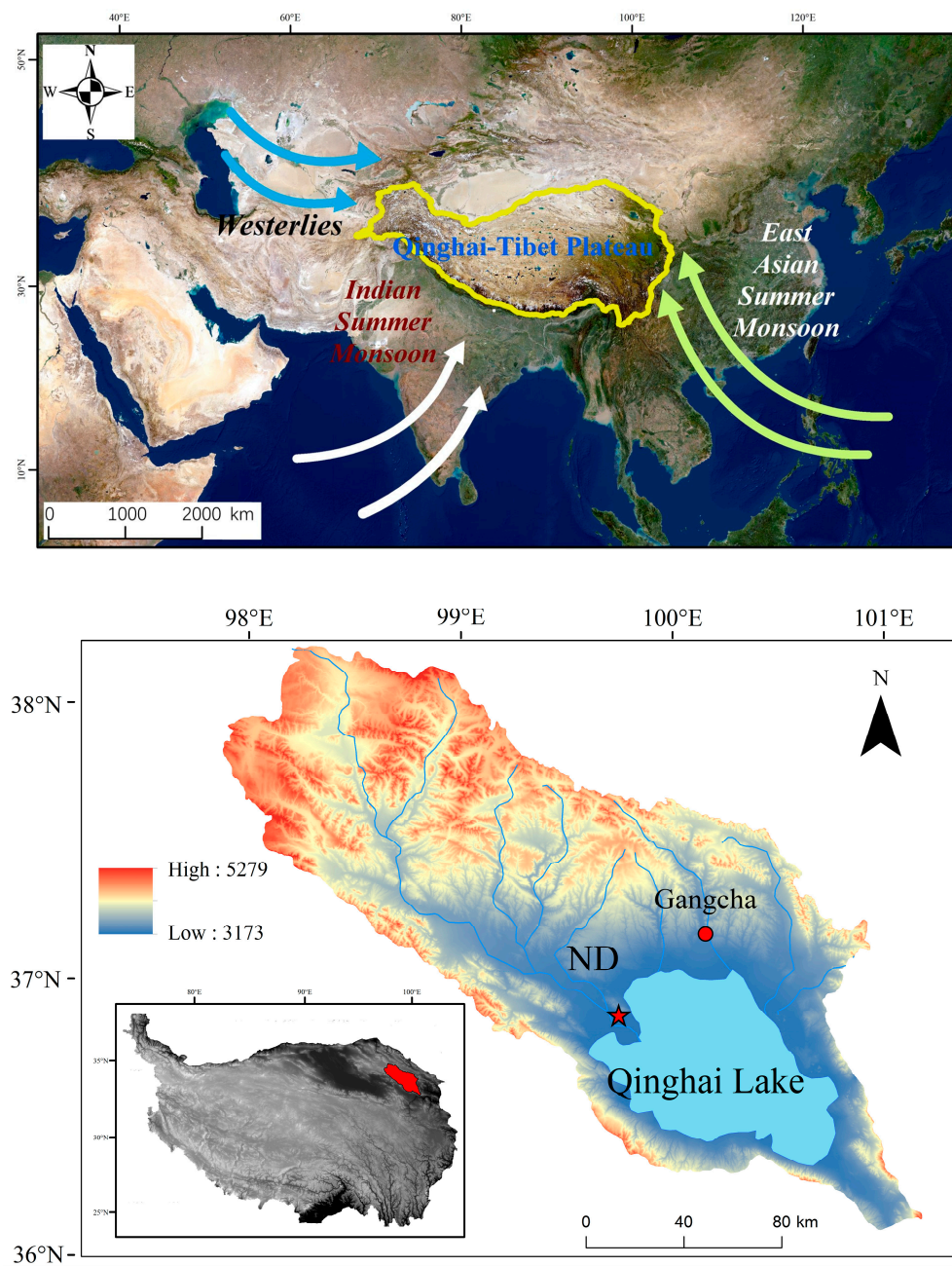


Figure 1. Map of the study area. The Qinghai-Tibet Plateau (QTP) is located in Central Asia, and the Qinghai Lake (QHL) Basin is located in the northeastern QTP, as indicated by the inset map. The red pentagon on the map denotes the location of the Niaodao (ND) profile examined in this study.

2.2. Samples and Analytical Methods

In this study, we specifically targeted the ND profile (37.04° N, 99.74° E, 3215 m) (Figure 1). The surface vegetation in this area is dominated by arid and semi-arid vegetation, including *Potentilla fruticosa* L., *Achnatherum splendens*, and *Stipa krylovii*. With a substantial thickness of approximately 600 cm, the ND profile was located on the second terrace of the Buha River. The uppermost 30 cm of this profile consisted of modern soil enriched with plant roots. At greater depths, that is, strata at 165–240 cm and 310–350 cm, we encountered two comparatively dark, compacted, erosion-defying sandy ancient paleosols [20] (Figure 2). We meticulously collected 95 bulk samples and 22 optically stimulated luminescence (OSL) samples within a height range of 0–475 cm. The OSL samples were used for age

testing, whereas the bulk samples were analyzed for TOC. Additionally, we selected 53 bulk samples at intervals of 5–15 cm for $\delta^{13}\text{C}_{\text{org}}$ testing.

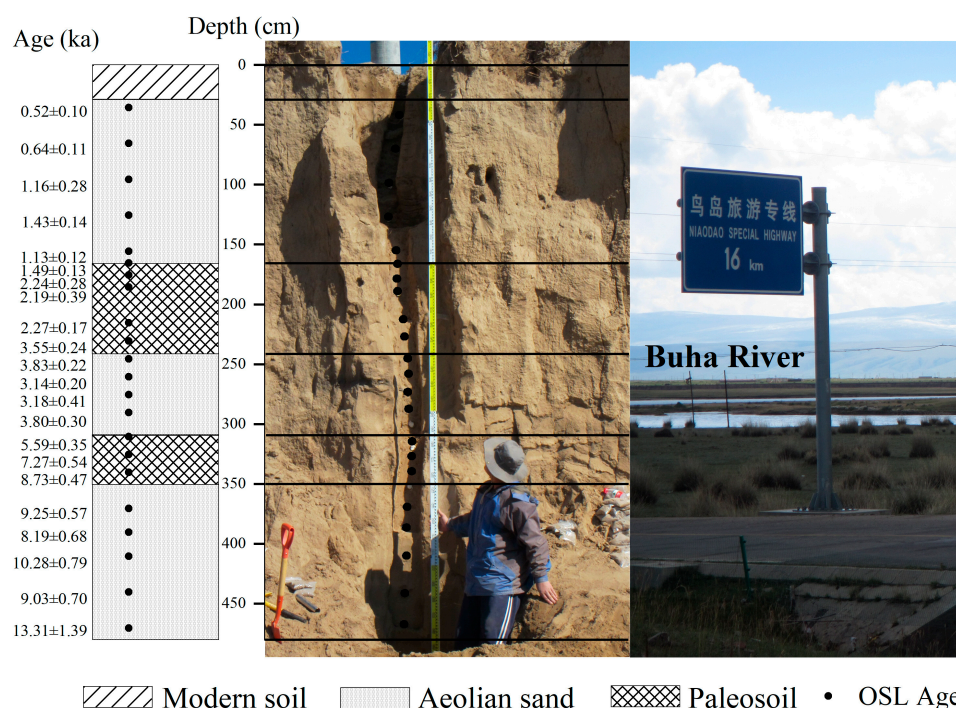


Figure 2. Stratigraphy and dating of the ND profile, with the age scale of the profile referenced to [20]; the ND profile is located along the Buha River.

Pretreatment and test analyses of the $\delta^{13}\text{C}_{\text{org}}$ sample were conducted at the Stable Isotope Laboratory at the Institute of Earth Environment, Chinese Academy of Sciences. The organic carbon samples were dried in an oven at 50 °C, and visible animal and plant residues were removed before grinding the samples to a 100 μm mesh size. To eliminate carbonates, approximately 3 g of the sample was reacted with excess (2 mol/L) hydrochloric acid at ambient temperature for one day. To achieve neutrality, the specimen was exhaustively rinsed with deionized water, subsequently dried at 40 °C, and further pulverized. The desiccated samples were incinerated within vacuum-sealed quartz tubes at 850 °C for a duration of 4 h, with 1 g each of CuO, Cu, and Pt foil. The resultant carbon dioxide was isolated via cryogenic purification. The isotopic ratios of the purified CO_2 were quantified using a Finnigan MAT 251 gas source mass spectrometer. These isotopic ratios are documented in δ -notation and articulated as per mil (‰) variances relative to the V-PDB benchmark for carbon [25]. Replicate analyses of the 53 samples showed an average standard deviation of 0.2‰. The experimental procedure is shown in Figure 3.

The pretreatment and analysis of TOC samples were conducted at the Qinghai Provincial Key Laboratory of Physical Geography and Environmental Processes, Qinghai Normal University. The samples were dried in an oven at 50 °C, and visible animal and plant residues were meticulously removed and ground to a 200 μm mesh. Approximately 0.3 g of samples was treated with 10% HCl at an ambient temperature. After completion of the reaction, the samples were washed repeatedly with deionized water until the pH exceeded 6. The samples were then dried at 40 °C and analyzed using a Vario TOC cube Analyzer [26]. The overall precision of the TOC analysis was less than 0.5%.

Analysis of χ_{lf} and M_z , along with OSL dating, was conducted at the Qinghai Provincial Key Laboratory of Physical Geography and Environmental Processes, Qinghai Normal University. Detailed information regarding the specific experimental process can be found in the relevant literature [20].

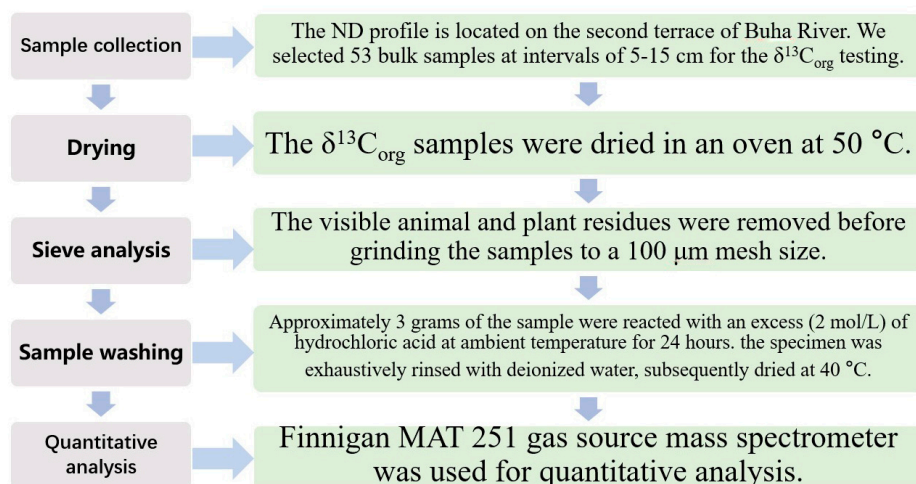


Figure 3. Experimental procedures for the $\delta^{13}\text{C}_{\text{org}}$ sample.

3. Results

In accordance with the results of the OSL dating [20], the profile predominantly documents the compositional features of the $\delta^{13}\text{C}_{\text{org}}$ and TOC in the aeolian sediment during the Holocene.

The ND profile suggested that the regional environmental changes from 11 ka to the present. During this period, the $\delta^{13}\text{C}_{\text{org}}$ values exhibited a range spanning from -25.24‰ to -22.72‰ , with an average of -23.58‰ . During the Early Holocene (11–9 ka), the $\delta^{13}\text{C}_{\text{org}}$ values ranged from -23.93‰ to -22.93‰ , averaging -23.30‰ . The Middle Holocene (9–4 ka) witnessed the $\delta^{13}\text{C}_{\text{org}}$ values varying between -23.43‰ and -22.72‰ , with an average of -23.19‰ . During the Late Holocene (4–0 ka), the $\delta^{13}\text{C}_{\text{org}}$ values spanned from -25.24‰ to -22.99‰ , with an average of -23.91‰ . From the overall trend of the curve, the $\delta^{13}\text{C}_{\text{org}}$ values exhibit significant fluctuations during the Early Holocene, gradually shifting towards positive values. Throughout the Middle Holocene, a predominantly positive trend persisted. However, beginning in the Late Holocene, a pronounced negative trend emerged (Figure 4a).

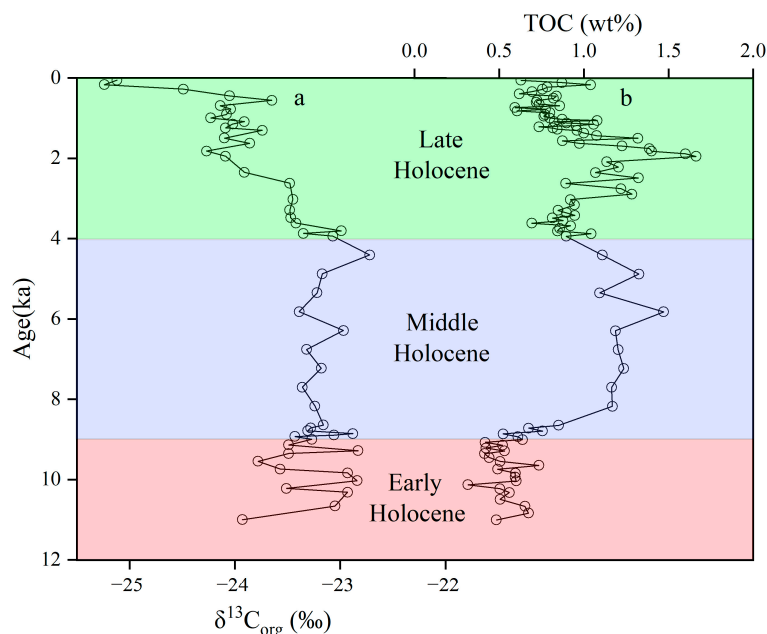


Figure 4. Data results are correlated with the age of the ND profile. (a) $\delta^{13}\text{C}_{\text{org}}$ and (b) total organic carbon (TOC).

From 11 ka to the present, the TOC values exhibited a range spanning from 0.32 to 1.66 wt%, with an average of 0.85 wt%. During the Early Holocene (11–9 ka), the TOC values ranged from 0.32 to 0.73 wt%, with an average of 0.52 wt%. During the Middle Holocene (9–4 ka), the TOC values ranged from 0.52 to 1.47 wt%, with an average of 1.00 wt%. The TOC values ranged from 0.59 to 1.66 wt%, with an average of 0.92 wt% during the Late Holocene (4–0 ka). Analyzing the overall trend throughout the Early Holocene, the TOC values were comparatively subdued, exhibiting a gradual ascent to reach a plateau of elevated levels throughout the Middle Holocene. The overall fluctuation range expanded significantly, the trend gradually decreased during the Late Holocene, and the TOC reached its peak at approximately 2 ka (Figure 4b).

4. Discussion

4.1. Terrestrial Ecosystem Is Not a Major Contributor to the Lake Organic Matter

The $\delta^{13}\text{C}_{\text{org}}$ values of the ND profile spanned from -25.24‰ to -22.72‰ , exhibiting a fluctuation amplitude of 2.52‰ . The Zhongyangchang (ZYC) aeolian profile is located at the southeastern margin of the QHL [19]. This profile is similar to the ND profile and can be divided stratigraphically from top to bottom into modern soil, loess containing a paleosol, and aeolian sand. The $\delta^{13}\text{C}_{\text{org}}$ values range from -25.8‰ to -24.8‰ , with an amplitude of 1‰ [19]. The $\delta^{13}\text{C}_{\text{org}}$ values of the two profiles had a small change. However, the variation range of the $\delta^{13}\text{C}_{\text{org}}$ in the sediment of QHL is between -30‰ and -20‰ , with an amplitude of 10‰ [2]. The aquatic plants are primarily dominated by *Cladophora* in modern QHL, and the $\delta^{13}\text{C}_{\text{org}}$ values ranged from -33.6‰ to -28.6‰ [4]. Genggahai Lake is a diminutive and superficial aquatic entity located in the Gonghe Basin in the northeastern QTP. The oscillation magnitude of $\delta^{13}\text{C}_{\text{org}}$ within the lacustrine sediment was approximately 12‰ [27] (Figure 5A). The $\delta^{13}\text{C}_{\text{org}}$ values of terrestrial ecosystems have changed slightly, whereas those of lacustrine ecosystems have significantly changed during the Holocene. Studies of the $\delta^{13}\text{C}_{\text{org}}$, $\delta^{15}\text{N}_{\text{tot}}$, and atomic $\text{C}_{\text{org}}/\text{N}_{\text{tot}}$ ratio of sediments from Lake Ximencuo in the eastern QTP show that the bulk organic matter in these lake sediments originates from a mixed source comprising autochthonous algae and aquatic and terrestrial plant inputs [28]. As inferred from the preceding analysis, irrespective of the lacustrine spatial extent, the content and variation of the $\delta^{13}\text{C}_{\text{org}}$ diverge from terrestrial ecosystem deposits. Terrestrial ecosystems were not the principal contributors to lacustrine organic matter during the Holocene.

Research has shown that TOC around the QHL undergoes little degradation in arid and cold climates [19,29]. The TOC values of the ND profile spanned from 0.32 to 1.66 wt%, whereas that of the ZYC profile range from 0.12 to 3.19 wt% [19]. TOC values were lower in the Early Holocene and higher in the Late Holocene. During the Early Holocene, the TOC values were low, whereas they were considerably elevated during the Middle and Late Holocene. However, the TOC values in lacustrine sediments of the QHL are higher than that in terrestrial sediments, ranging from 0.4 to 9.0 wt%. Its trend was higher at 10.5–4 ka, and its content decreased after 4 ka [2]. The TOC values of the Genggahai Lake sediments were significantly higher than those of the terrestrial sediments [27] (Figure 5B). The TOC content and its variations in the terrestrial aeolian and lacustrine sediments indicate that the organic matter sources of the sediments from Genggahai and QHL were not primarily derived from terrestrial ecosystems during the Holocene. In the Early Holocene, the lake water level was low [4], the summer monsoon was enhanced, the summer sunshine duration was long [1,4], and the algae (mainly *Cladophora*) in the lake increased. In the Middle and Late Holocene, the water level was several meters higher than it is now [30], and algae (mainly *Cladophora*) became the dominant contributor to lacustrine organic matter [31], resulting in more negative $\delta^{13}\text{C}_{\text{org}}$ values in lacustrine sediments. Therefore, the organic matter in the lacustrine sediments of the QHL may have been derived from aquatic organisms.

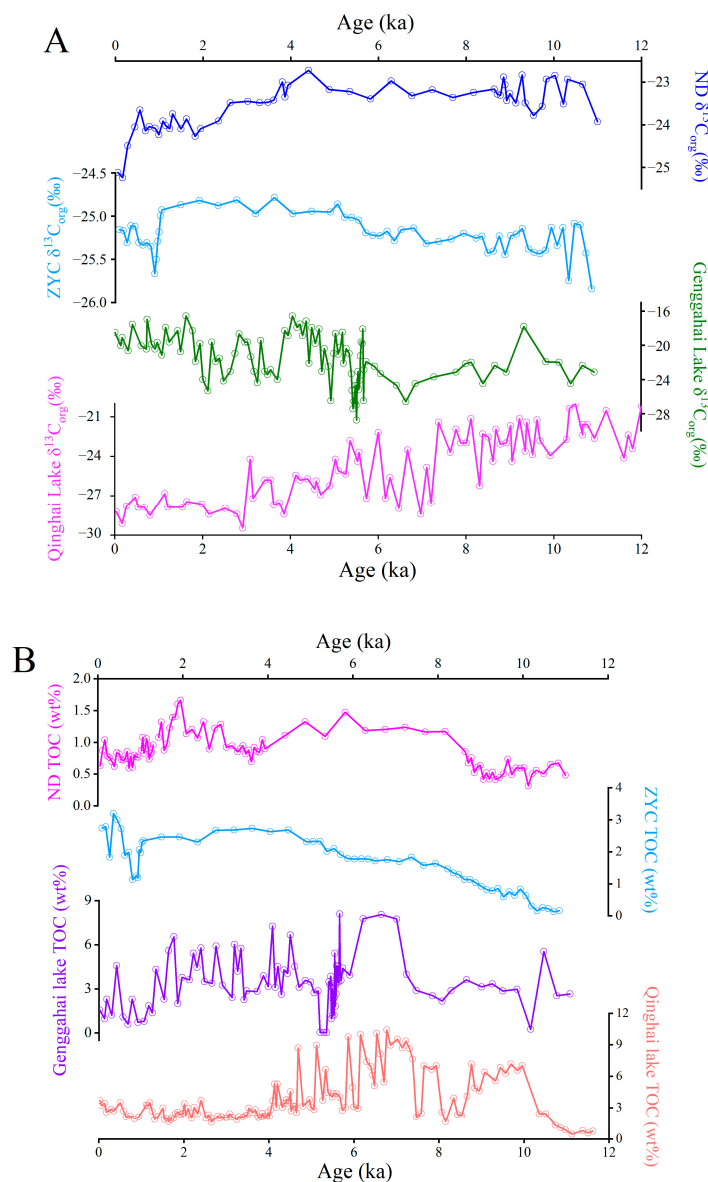


Figure 5. Numerical comparison of the $\delta^{13}C_{org}$ (A) and TOC (B) in terrestrial (ND profile and ZYC profile) and lacustrine sediments (Genggahai Lake and QHL).

4.2. The Impact of Temperature on the $\delta^{13}C_{org}$ Values

In the study of the relationship between modern vegetation and $\delta^{13}C_{org}$ values, the soil $\delta^{13}C_{org}$ values have been observed to be $\leq -24\text{‰}$ when the prevalence of the C_3 vegetation is at its maximum (100%), and the soil $\delta^{13}C_{org}$ values are $\geq -14\text{‰}$ when the dominance of the C_4 vegetation is absolute (100%) [32]. The $\delta^{13}C_{org}$ values of the ND profile ranged from -25.24‰ to -22.72‰ , with an average of -23.58‰ . Researchers have found that the isotopic fractionation occurring during the metamorphosis of vegetal remnants into organic matter after deposition may lead to a $\delta^{13}C_{org}$ matter change of approximately 1‰ [33]. Therefore, the $\delta^{13}C_{org}$ values of vegetation in the ND profile should be between -26.24‰ and -23.72‰ , with an average of -24.58‰ . The vegetation composition of the ND profile was predominantly C_3 species, with the influence of C_4 species largely overlooked during the Holocene. The fluctuation in the $\delta^{13}C_{org}$ values of the ND profile primarily reflects the reaction of the C_3 vegetation to the climatic conditions, rather than the change in the relative abundance of the C_3 and C_4 vegetation.

Numerous elements can potentially impact the composition of the $\delta^{13}C_{org}$ values of vegetation with the most important being atmospheric CO_2 concentration, precipitation,

and temperature [17,21,34]. Research shows that for every 100 ppmv increase in atmospheric CO₂ concentration, the $\delta^{13}\text{C}_{\text{org}}$ of vegetations decreases by 2‰ [35]. During the Holocene, the overall change range is 20 ppmv, indicating that the influence of atmospheric CO₂ concentration changes on the composition of $\delta^{13}\text{C}_{\text{org}}$ is approximately 0.4‰ [36]. The variation range of the $\delta^{13}\text{C}_{\text{org}}$ values recorded by aeolian sediment in the ND profile is approximately 2.5‰. The change in CO₂ concentration is not primarily influencing the $\delta^{13}\text{C}_{\text{org}}$ values of $\delta^{13}\text{C}_{\text{org}}$ plants. Numerous studies have shown that the relative humidity, as well as the amount of precipitation, is negatively relative to the $\delta^{13}\text{C}_{\text{org}}$ of terrestrial plants [37,38]. Based on the quantitative study of the carbon isotope composition of C₃ plants and precipitation in Northern China, the average carbon isotope composition of C₃ plants decreased by approximately 0.49‰ for every 100 mm increase in precipitation [38]. During the late Holocene, the $\delta^{13}\text{C}_{\text{org}}$ value of the ND section decreased by 1.25‰, and the precipitation increased by about 255 mm, which was inconsistent with the gradual decrease in precipitation in the Late Holocene [39] (Figure 6b). Therefore, precipitation is not a climatic factor affecting the $\delta^{13}\text{C}_{\text{org}}$ values of the aeolian sediments in the QHL Basin since the Holocene.

Through extensive research on modern surface soil $\delta^{13}\text{C}_{\text{org}}$ across the QTP, the $\delta^{13}\text{C}_{\text{org}}$ values have been observed to be predominantly influenced by temperature and precipitation [21,40,41]. In Northern China, the study of C₃ plants in the 400 mm annual average precipitation isohaline has discovered a significant positive correlation between the $\delta^{13}\text{C}_{\text{org}}$ values of C₃ plants and the annual average temperature [21]. The Gangcha weather station, situated 50 km from the ND profile, recorded a mean annual precipitation of 370 mm between 1975 and 2011 [20]. The ND profile was located near the QHL, and the climatic conditions were similar to those at Gangcha station. The $\delta^{13}\text{C}_{\text{org}}$ values in aeolian sediments may be influenced by petrogenic carbon [42]. In the study of $\delta^{13}\text{C}_{\text{org}}$ in loess since the Last Glacial Period in Northwest China, the $\delta^{13}\text{C}_{\text{org}}$ of loess falls into roughly the same value range as that of parent rocks in the dust source area [43]. The ND profile is also in this study area, and therefore the $\delta^{13}\text{C}_{\text{org}}$ of parent rocks has less influence on the isotopes of sediments.

The significance of $\delta^{13}\text{C}_{\text{org}}$ in soils is consistent with the plant. Research shows that the $\delta^{13}\text{C}_{\text{org}}$ composition of C₃ plants is more strongly influenced by temperature in arid and semi-arid regions [44–46]. Thus, temperature may be the principal factor influencing the soils' $\delta^{13}\text{C}_{\text{org}}$ values in the studied region. The researchers have found that the $\delta^{13}\text{C}_{\text{org}}$ and $\delta^{15}\text{N}_{\text{tot}}$ proxies of the lacustrine sediment record air temperature variations in the growing season in the Ximencuo Lake area [28]. Other researchers have found that the variation of $\delta^{13}\text{C}_{\text{org}}$ values in a Holocene loess profile, located in the eastern Hunshandake Sandy Land, showed significant positive correlations with accumulated temperatures above 10 and 0 °C [16]. The $\delta^{13}\text{C}_{\text{org}}$ variability within the ND profile exhibits limited amplitude, suggesting that vegetation composition in this region has undergone minimal alterations, and the ecosystem remains relatively stable during the Holocene. The modern ecosystem near the ND profile is a temperate steppe and desert. Therefore, we used $\delta^{13}\text{C}_{\text{org}}$ analysis of the ND profile as a proxy of temperature change in the QHL Basin.

In this study, the $\delta^{13}\text{C}_{\text{org}}$ of the ND profile was compared with the summer temperature of the QHL alkenone record during the Holocene [47]. We found that the $\delta^{13}\text{C}_{\text{org}}$ is different from the above temperature reconstruction, but the general trend is consistent. However, the comparison of the $\delta^{13}\text{C}_{\text{org}}$ and East Asian temperatures inferred from brGDGTs in loess [48]; the summer temperatures in Northern China reconstructed by integrating instrumental data, proxy records, and model simulations [49]; and the global temperature anomaly from 73 globally distributed records [50] reveal a substantial degree of similarity (Figure 5). This may be due to the lake reservoir effect, which has been noted across numerous lacustrine sediments, particularly in the cold and dry lakes in the northeast of QTP [2,12]. Aeolian sediments have certain limitations, such as low temporal resolution and discontinuous deposition. During the Middle Holocene, sedimentation rates were low, resulting in challenges in representing the finer details of the ND profile [20].

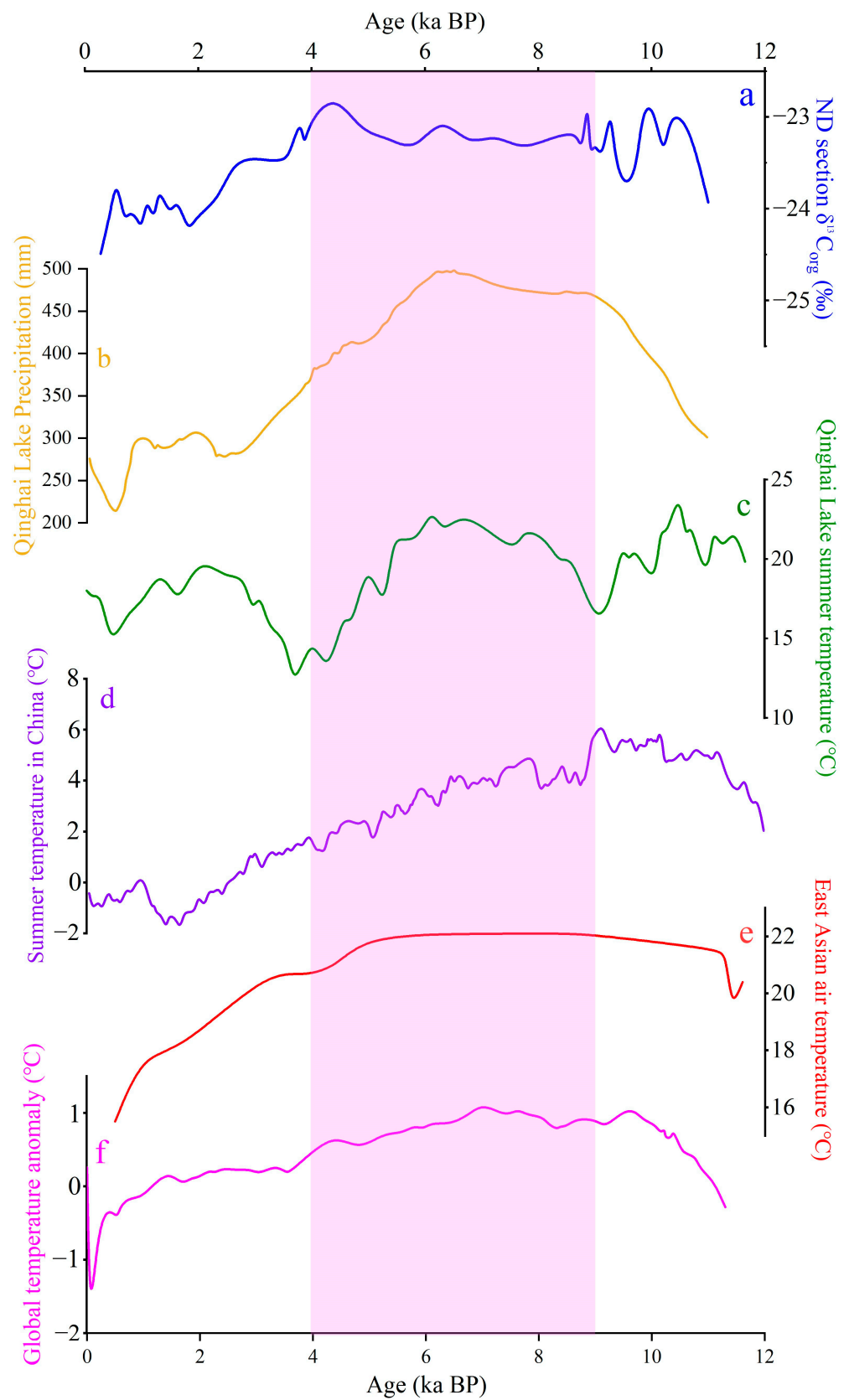


Figure 6. Comparison of the $\delta^{13}\text{C}_{\text{org}}$ in the ND profile of QHL with other indicators during the Holocene. (a) The $\delta^{13}\text{C}_{\text{org}}$ of the ND profile, (b) the quantitative precipitation reconstruction of QHL [39], (c) the summer temperature of QHL [47], (d) the reconstruction of summer temperature of China [49], (e) the East Asian air temperature [48], and (f) the global temperature [50].

4.3. Temperature Changes in QHL Basin during the Holocene Recorded in the ND Profile

In many studies in Northern China, the $\delta^{13}\text{C}_{\text{org}}$ values of C_3 plants have been found to exhibit a significant positive correlation with temperature [21,51]. When the temperature decreases, the loss of water evaporation decreases and the fractionation of carbon isotopes increases; thus, the carbon isotopes of plants decrease [37]. This study reconstructed the temperature record in the area by employing a comprehensive analysis of the $\delta^{13}\text{C}_{\text{org}}$ and TOC analysis, in conjunction with a high-resolution chronological framework, the χ_{lf} and the Mz [20]. These conventional proxy indices were compared with the Northern Hemisphere summer insolation at 37°N [52] during the Holocene (Figure 7). The $\delta^{13}\text{C}_{\text{org}}$ values observed in the ND profile exhibited a strong concordance with the Northern Hemisphere summer insolation at 37°N . The impact of summer insolation on temperature subsequently influences the $\delta^{13}\text{C}_{\text{org}}$ of vegetations. Additionally, the $\delta^{13}\text{C}_{\text{org}}$ values in the soils are influenced by the $\delta^{13}\text{C}_{\text{org}}$ values of the local vegetation [32]. The effect of temperature variation on the fractionation processes of different plant species is accurately recorded within the plant body, resulting in changes in both plant and soil $\delta^{13}\text{C}_{\text{org}}$ values [16]. Therefore, the temperature changes during the Holocene around the QHL Basin have been reconstructed through analyzing the $\delta^{13}\text{C}_{\text{org}}$ in the ND profile.

During the Early Holocene, the χ_{lf} was at its lowest, indicating reduced pedogenesis, and the Mz was substantial and exhibited pronounced fluctuations, indicating the wind conditions were characterized by their strong, unstable, and recurrent nature (Figure 7). Dry climate conditions are suggested by the low χ_{lf} and high Mz [20]. Several studies have been conducted on different environmental proxy indicators in aeolian sediments from this period and have inferred that evaporation was intense, the moisture required for vegetation was insufficient, and aeolian activity was pronounced [12,53]. The temperature in the QHL Basin was higher, albeit with notable fluctuations. Therefore, the initial TOC diminished, and the soil TOC value decreased. During the Middle Holocene, the χ_{lf} was at its finest, it was primarily composed of silt, and the rate of sand deposition was at a minimum, suggesting a transition to stable warm and wet conditions (Figure 7). An examination of the salinity proxies from the paleo-shoreline and waters of the QHL revealed climatic conditions characterized by warmth and humidity during this period [30], which agrees with the conclusions drawn from the research presented in this study. During this stage, the temperature remains consistently high and stable. Aeolian activity was subdued, whereas pedogenesis intensity increased [20,54], resulting in a substantial accumulation of TOC. During the Late Holocene, indications of an unstable climate were evidenced by a marked decrease in χ_{lf} and roughening of Mz (Figure 7). These signs indicated an intensification of aeolian activity and a shift towards a climate that is both colder and more arid. There was a rapid decline in temperature accompanied by intensified aeolian activity [20,55]. There was a significant decline in temperature during this period [53,54], coinciding with an increase in aeolian activity. The χ_{lf} and Mz indicate the partial development of paleosol at approximately 2 ka, leading to an increase in TOC. Subsequent to approximately 2 ka, there was a noted reduction in χ_{lf} , coupled with a coarsening of Mz. These changes signal an intensification of aeolian activity, indicating a shift towards increasingly arid and cold climatic conditions. The research findings indicate that the climatic conditions became colder and drier, further intensifying aeolian activity [53,54]. Based on the above analysis, during the Early Holocene, the temperature increased with high frequency and amplitude oscillations, strong aeolian activity, and low TOC accumulation. During the Middle Holocene, the temperature remained high and stable with the weakest aeolian activity and intensified pedogenesis. During the Late Holocene, the temperature decreased at a high rate, with renewed aeolian activity and weak pedogenesis. The climatic system exhibits greater complexity in the QHL Basin of the QPT, situated at the periphery of the EASM and ISM influences, compared to other sectors of the QPT. This is probably due to the complicated interaction between the EASM and ISM.

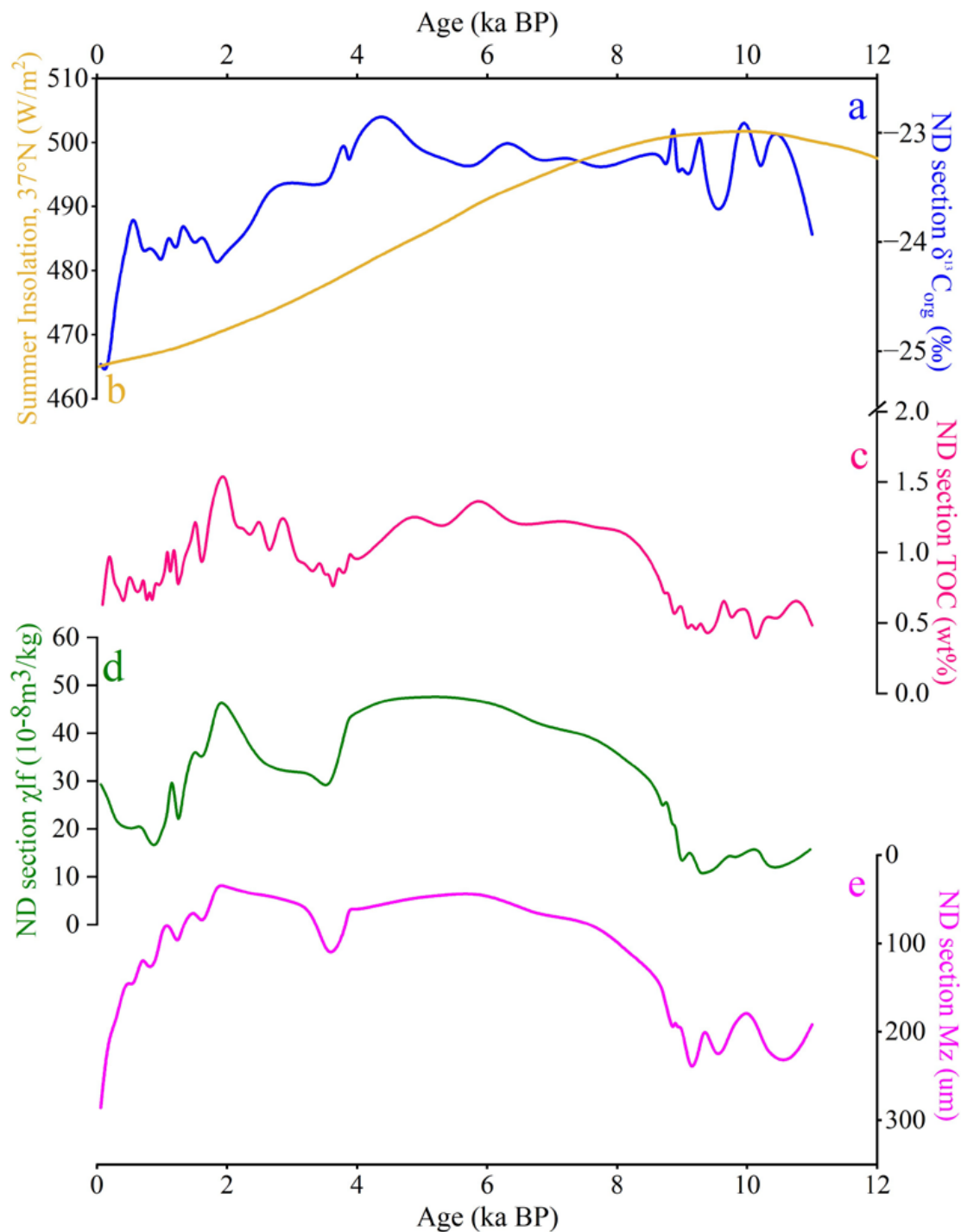


Figure 7. Comparison of the $\delta^{13}\text{C}_{\text{org}}$ in the ND profile of QHL with other indicators since the Holocene. (a) The $\delta^{13}\text{C}_{\text{org}}$ of the ND profile, (b) the Northern Hemisphere summer insolation at 37°N [52], (c) the TOC, (d) low-frequency magnetic susceptibility (χ_{lf}), and (e) median grain size (M_z) of the ND profile. (d,e) Have been published in detail in the literature [20].

In the study of the relationship between the temperature and $\delta^{13}\text{C}_{\text{org}}$ of surface soil, the $\delta^{13}\text{C}_{\text{org}}$ values have been observed to elucidate the relationship between these two variables, providing insights into paleoenvironmental reconstruction [16]. Therefore, surface soil $\delta^{13}\text{C}_{\text{org}}$ will be collected in subsequent research. We attempt to quantitatively reconstruct Holocene seasonal and accumulated temperatures in the QHL Basin based on $\delta^{13}\text{C}_{\text{org}}$

changes in an aeolian profile using the surface soil $\delta^{13}\text{C}_{\text{org}}$ dataset and high-resolution modern climate reanalysis data.

5. Conclusions

Based on the study of the TOC and $\delta^{13}\text{C}_{\text{org}}$ in the Niaodao (ND) profile, this study further extends the applicability of the $\delta^{13}\text{C}_{\text{org}}$ indicator in paleoclimate reconstruction. The variation trend and amplitude of the TOC and $\delta^{13}\text{C}_{\text{org}}$ in aeolian and lacustrine sediments are found to be different. The terrestrial ecosystem was not a principal contributor to lacustrine organic matter within the northeastern QTP during the Holocene.

The change in $\delta^{13}\text{C}_{\text{org}}$ values in the ND profile primarily reflects the response of C_3 plants to environmental factors. The $\delta^{13}\text{C}_{\text{org}}$ values of C_3 plants are primarily influenced by temperature. During the Holocene, variations in the $\delta^{13}\text{C}_{\text{org}}$ values in the ND profile serve as an indicator of temperature fluctuations in the QHL Basin.

During the Early Holocene, the temperature increased with relatively high frequency and amplitude oscillations, strong aeolian activity, and low TOC accumulation. During the Middle Holocene, the temperature remained relatively high and stable with the weakest aeolian activity and intensified pedogenesis. During the Late Holocene, the temperature decreased at a relatively high rate, with renewed aeolian activity and weak pedogenesis.

Author Contributions: Conceptualization, C.E.; methodology, X.L.; software, Z.Z.; validation, X.J.; formal analysis, J.Z.; investigation, Q.P. and Y.S. (Yunkun Shi); data curation, S.Z.; writing—original draft preparation, Q.P.; writing—review and editing, C.E.; supervision, Y.S. (Yongjuan Sun). All authors have read and agreed to the published version of the manuscript.

Funding: This research was funded by the National Natural Science Foundation of China (grant no. 42171011) and the Natural Science Foundation of the Qinghai Provincial Science and Technology Department (grant no. 2021-ZJ-918).

Institutional Review Board Statement: Not applicable.

Informed Consent Statement: Not applicable.

Data Availability Statement: The data presented in this study are available on request from the corresponding author. The data are not publicly available due to privacy.

Acknowledgments: We would like to thank Yongxin Zeng, Qi Zhang, Jie Zhang, and Xianyu Cao for their help with field and laboratory work. We would also like to thank Manping Sun for his valuable suggestions. Special thanks go to the anonymous reviewers and editors, whose constructive suggestions and useful comments helped clarify and improve the quality of the paper.

Conflicts of Interest: The authors declare no conflicts of interest.

References

1. An, Z.S.; Colman, S.M.; Zhou, W.; Li, X.; Brown, E.T.; Jull, A.T.; Cai, Y.; Huang, Y.; Lu, X.; Chang, H.; et al. Interplay between Westerlies and Asian monsoon recorded in Lake Qinghai sediments since 32 ka. *Sci. Rep.* **2012**, *2*, 619. [[CrossRef](#)] [[PubMed](#)]
2. Ji, S.; Xingqi, L.; Sumin, W.; Matsumoto, R. Palaeoclimatic changes in the Qinghai Lake area during the last 18,000 years. *Quat. Int.* **2005**, *136*, 131–140. [[CrossRef](#)]
3. Wang, Y.; Shen, J.; Xu, X.; Liu, X.; Sirocko, F.; Zhang, E.; Ji, J. Environmental changes during the past 13500 cal. a BP deduced from lacustrine sediment records of Lake Qinghai, China. *Chin. J. Geochem.* **2011**, *30*, 479–489. [[CrossRef](#)]
4. Liu, W.G.; Li, X.Z.; An, Z.S.; Xu, L.; Zhang, Q. Total organic carbon isotopes: A novel proxy of lake level from Lake Qinghai in the Qinghai–Tibet Plateau, China. *Chem. Geol.* **2013**, *347*, 153–160. [[CrossRef](#)]
5. Herzschuh, U.; Borkowski, J.; Schewe, J.; Mischke, S.; Tian, F. Moisture-advection feedback supports strong early-to-mid Holocene monsoon climate on the eastern Tibetan Plateau as inferred from a pollen-based reconstruction. *Palaeogeogr. Palaeoclimatol. Palaeoecol.* **2014**, *402*, 44–54. [[CrossRef](#)]
6. Li, L.; Zhang, F.P.; Feng, Q.; Wang, H.W.; Wei, Y.F.; Li, X.J.; Nie, S.; Liu, J.Y. Responses of grassland to climate change and human activities in the area around Qinghai Lake. *Chin. J. Ecol.* **2019**, *38*, 1157.
7. Li, H.; Liu, X.; Tripathi, A.; Feng, S.; Kelley, A.M. Factors controlling the oxygen isotopic composition of lacustrine authigenic carbonates in western china: Implications for paleoclimate reconstructions. *Sci. Rep.* **2020**, *10*, 16370. [[CrossRef](#)] [[PubMed](#)]

8. Sha, Z.; Wang, Q.; Wang, J.; Du, J.; Hu, J.; Ma, Y.; Kong, F.; Wang, Z. Regional environmental change and human activity over the past hundred years recorded in the sedimentary record of Lake Qinghai, China. *Environ. Sci. Pollut. Res.* **2017**, *24*, 9662–9674. [[CrossRef](#)]
9. Liu, W.G.; Li, X.Z.; Wang, Z.; Wang, H.; Liu, H.; Zhang, B.; Zhang, H. Carbon isotope and environmental changes in lakes in arid Northwest China. *Sci. China Earth Sci.* **2019**, *62*, 1193–1206. [[CrossRef](#)]
10. Hou, J.; D'Andrea, W.J.; Liu, Z. The influence of ^{14}C reservoir age on interpretation of paleolimnological records from the Tibetan Plateau. *Quat. Sci. Rev.* **2012**, *48*, 67–79. [[CrossRef](#)]
11. Chongyi, E.; Sun, Y.J.; Liu, X.J.; Hou, G.L.; Lv, S.C.; Yuan, J.; Sun, M.P. A comparative study of radiocarbon dating on terrestrial organisms and fish from Qinghai Lake in the northeastern Tibetan Plateau, China. *Holocene* **2018**, *28*, 1712–1719. [[CrossRef](#)]
12. Chen, F.H.; Wu, D.; Chen, J.; Zhou, A.; Yu, J.; Shen, J.; Wang, S.; Huang, X. Holocene moisture and East Asian summer monsoon evolution in the northeastern Tibetan Plateau recorded by Lake Qinghai and its environs: A review of conflicting proxies. *Quat. Sci. Rev.* **2016**, *154*, 111–129. [[CrossRef](#)]
13. Rao, Z.G.; Chen, F.H.; Cheng, H.; Liu, W.G.; Wang, G.A.; Lai, Z.P.; Bloemendal, J. High-resolution summer precipitation variations in the western Chinese Loess Plateau during the last glacial. *Sci. Rep.* **2013**, *3*, 2785. [[CrossRef](#)] [[PubMed](#)]
14. Yang, S.; Liu, L.; Chen, H.; Tang, G.; Luo, Y.; Liu, N.; Cheng, T.; Li, D. Variability and environmental significance of organic carbon isotopes in Ganzi loess since the last interglacial on the eastern Tibetan Plateau. *Catena* **2021**, *196*, 104866. [[CrossRef](#)]
15. Mansour, A.; Wagreich, M. Earth system changes during the cooling greenhouse phase of the Late Cretaceous: Coniacian-Santonian OAE3 subevents and fundamental variations in organic carbon deposition. *Earth-Sci. Rev.* **2022**, *229*, 104022. [[CrossRef](#)]
16. Zeng, Y.; Li, X.S.; Liu, Y.J.; Li, Y.F.; Qin, L.S.; Zhao, C.; Liu, M.H.; Zhou, Y.W.; Han, Z.Y.; Wang, Y.; et al. Quantification of Holocene temperatures in the eastern Hunshandake Sandy Land using $\delta^{13}\text{C}$ of loess organic matter. *Glob. Planet. Change* **2024**, *237*, 104457. [[CrossRef](#)]
17. Li, X.Z.; Liu, X.J.; He, Y.; Liu, W.; Zhou, X.; Wang, Z. Summer moisture changes in the Lake Qinghai area on the northeastern Tibetan Plateau recorded from a meadow section over the past 8400 yrs. *Glob. Planet. Change* **2018**, *161*, 1–9. [[CrossRef](#)]
18. Yuan, B.; Chen, K.; JM, B.; Ye, S. The formation and evolution of the Qinghai Lake. *Quat. Sci.* **1990**, *10*, 233–243.
19. Zeng, F.M.; Liu, X.J.; Li, X.Z.; E, C.Y. Aquatic species dominate organic matter in Qinghai Lake during the Holocene: Evidence from eolian deposits around the lake. *J. Earth Sci.* **2017**, *28*, 484–491. [[CrossRef](#)]
20. Chongyi, E.; Zhang, J.; Chen, Z.Y.; Sun, Y.J.; Zhao, Y.J.; Li, P.; Sun, M.P.; Shi, Y.K. High resolution OSL dating of aeolian activity at Qinghai Lake, Northeast Tibetan Plateau. *Catena* **2019**, *183*, 104180. [[CrossRef](#)]
21. Wang, G.; Li, J.; Liu, X.; Li, X. Variations in carbon isotope ratios of plants across a temperature gradient along the 400 mm isoline of mean annual precipitation in north China and their relevance to paleovegetation reconstruction. *Quat. Sci. Rev.* **2013**, *63*, 83–90. [[CrossRef](#)]
22. Liu, X.; Su, Q.; Li, C.; Zhang, Y.; Wang, Q. Responses of carbon isotope ratios of C_3 herbs to humidity index in northern China. *Turk. J. Earth Sci.* **2014**, *23*, 100–111. [[CrossRef](#)]
23. Cheng, J.; Liu, C.H.; Liu, K.; Wu, J.S.; Fan, C.Y.; Xue, B.; Ma, R.H.; Song, C.Q. Potential impact of the dramatical expansion of Lake Qinghai on the habitat facilities and grassland since 2004. *J. Lake Sci.* **2021**, *33*, 922–934.
24. Zhiyong, D.; Ruijie, L.; Chang, L.; Chenxi, D. Temporal change characteristics of climatic and its relationships with atmospheric circulation patterns in Qinghai Lake Basin. *Adv. Earth Sci.* **2018**, *33*, 281.
25. Rao, Z.G.; Xu, Y.; Xia, D.; Xie, L.; Chen, F. Variation and paleoclimatic significance of organic carbon isotopes of Ili loess in arid Central Asia. *Org. Geochem.* **2013**, *63*, 56–63. [[CrossRef](#)]
26. Schumacher, B.A. *Methods for the Determination of Total Organic Carbon (TOC) in Soils and Sediments*; US Environmental Protection Agency, Office of Research and Development, Ecological Risk Assessment Support Center: Washington, DC, USA, 2002.
27. Qiang, M.R.; Chen, F.H.; Song, L.; Liu, X.; Li, M.; Wang, Q. Late quaternary aeolian activity in Gonghe Basin, northeastern Qinghai-Tibetan plateau, China. *Quat. Res.* **2013**, *79*, 403–412. [[CrossRef](#)]
28. Pu, Y.; Nace, T.; Meyers, P.A.; Zhang, H.; Wang, Y.; Zhang, C.; Shao, X. Paleoclimate changes of the last 1000 yr on the eastern qinghai-tibetan plateau recorded by elemental, isotopic, and molecular organic matter proxies in sediment from glacial lake ximencuo. *Palaeogeogr. Palaeoclimatol. Palaeoecol.* **2013**, *379–380*, 39–53. [[CrossRef](#)]
29. Xiao, J.; Nakamura, T.; Lu, H.; Zhang, G. Holocene climate changes over the desert/loess transition of north-central China. *Earth Planet. Sci. Lett.* **2002**, *197*, 11–18. [[CrossRef](#)]
30. Liu, X.J.; Lai, Z.P.; Madsen, D.; Zeng, F.M. Last deglacial and holocene lake level variations of qinghai lake, north-eastern qinghai-tibetan plateau. *J. Quat. Sci.* **2015**, *30*, 245–257. [[CrossRef](#)]
31. Li, X.Z.; Liu, W.G.; Xu, L. Evaluation of lacustrine organic $\delta^{13}\text{C}$ as a lake-level indicator: A case study of lake qinghai and the satellite lakes on the tibetan plateau. *Palaeogeogr. Palaeoclimatol. Palaeoecol.* **2019**, *532*, 109274. [[CrossRef](#)]
32. Tieszen, L.L.; Reed, B.C.; Bliss, N.B.; Wylie, B.K.; DeJong, D.D. NDVI, C_3 and C_4 production, and distributions in Great Plains grassland land cover classes. *Ecol. Appl.* **1997**, *7*, 59–78.
33. Melillo, J.M.; Aber, J.D.; Linkins, A.E.; Ricca, A.; Fry, B.; Nadelhoffer, K.J. Carbon and nitrogen dynamics along the decay continuum: Plant litter to soil organic matter. *Plant Soil* **1989**, *115*, 189–198. [[CrossRef](#)]
34. Wendler, I. A critical evaluation of carbon isotope stratigraphy and biostratigraphic implications for late cretaceous global correlation. *Earth-Sci. Rev.* **2013**, *126*, 116–146. [[CrossRef](#)]

35. Feng, X.; Epstein, S. Carbon isotopes of trees from arid environments and implications for reconstructing atmospheric CO₂ concentration. *Geochim. Cosmochim. Acta* **1995**, *59*, 2599–2608. [[CrossRef](#)]
36. Petit, J.R.; Jouzel, J.; Raynaud, D.; Barkov, N.I.; Barnola, J.M.; Basile, I.; Bender, M.; Chappellaz, J.; Davis, M.; Delaygue, G.; et al. Climate and atmospheric history of the past 420,000 years from the Vostok ice core, Antarctica. *Nature* **1999**, *399*, 429–436. [[CrossRef](#)]
37. Farquhar, G.; O’Leary, M.; Berry, J. On the relationship between carbon isotope discrimination and the intercellular carbon dioxide concentration in leaves. *Funct. Plant Biol.* **1982**, *9*, 121–137. [[CrossRef](#)]
38. Wang, G.A.; Han, J.; Liu, D. The carbon isotope composition of C3 herbaceous plants in loess area of northern China. *Sci. China Ser. D Earth Sci.* **2003**, *46*, 1069–1076. [[CrossRef](#)]
39. Herzschuh, U.; Birks, H.J.B.; Liu, X.; Kubatzki, C.; Lohmann, G. What caused the mid-holocene forest decline on the eastern tibet-qinghai plateau? *Glob. Ecol. Biogeogr.* **2010**, *19*, 278–286. [[CrossRef](#)]
40. Lu, H.; Wu, N.; Gu, Z.; Guo, Z.; Wang, L.; Wu, H.; Wang, G.; Zhou, L.; Han, J.; Liu, T. Distribution of carbon isotope composition of modern soils on the Qinghai-Tibetan Plateau. *Biogeochemistry* **2004**, *70*, 275–299. [[CrossRef](#)]
41. Zhao, Y.; Wu, F.; Fang, X.; Yang, Y. Altitudinal variations in the bulk organic carbon isotopic composition of topsoil in the Qilian Mountains area, NE Tibetan Plateau, and its environmental significance. *Quat. Int.* **2017**, *454*, 45–55. [[CrossRef](#)]
42. Xie, S.; Guo, J.; Huang, J.; Chen, F.; Wang, H.; Farrimond, P. Restricted utility of $\delta^{13}\text{C}$ of bulk organic matter as a record of paleovegetation in some loess/paleosol sequences in the Chinese loess plateau. *Quat. Res.* **2004**, *62*, 86–93. [[CrossRef](#)]
43. Liu, W.G.; Yang, H.; Ning, Y.; An, Z. Contribution of inherent organic carbon to the bulk $\delta^{13}\text{C}$ signal in loess deposits from the arid western Chinese Loess Plateau. *Org. Geochem.* **2007**, *38*, 1571–1579. [[CrossRef](#)]
44. Wang, X.; Cui, L.; Xiao, J.; Ding, Z. Stable carbon isotope of black carbon in lake sediments as an indicator of terrestrial environmental changes: An evaluation on paleorecord from Daihai Lake, Inner Mongolia, China. *Chem. Geol.* **2013**, *347*, 123–134. [[CrossRef](#)]
45. Liu, X.; Colman, S.M.; Brown, E.T.; Henderson, A.C.; Werne, J.P.; Holmes, J.A. Abrupt deglaciation on the northeastern Tibetan Plateau: Evidence from Lake Qinghai. *J. Paleolimnol.* **2014**, *51*, 223–240. [[CrossRef](#)]
46. Zhang, Z.; Ullah, I.; Wang, Z.; Ma, P.; Zhao, Y.; Ma, X.; Li, Y. Reconstruction of temperature for the past 400 years in the Southern Margin of the Taklimakan Desert based on carbon isotope fractionation of Tamarix leaves. *Appl. Ecol. Environ. Res.* **2019**, *17*, 1. [[CrossRef](#)]
47. Hou, J.Z.; Huang, Y.; Zhao, J.; Liu, Z.; Colman, S.; An, Z. Large Holocene summer temperature oscillations and impact on the peopling of the northeastern Tibetan Plateau. *Geophys. Res. Lett.* **2016**, *43*, 1323–1330. [[CrossRef](#)]
48. Peterse, F.; Martínez-García, A.; Zhou, B.; Beets, C.J.; Prins, M.A.; Zheng, H.; Eglinton, T.I. Molecular records of continental air temperature and monsoon precipitation variability in East Asia spanning the past 130,000 years. *Quat. Sci. Rev.* **2014**, *83*, 76–82. [[CrossRef](#)]
49. Shi, F.; Lu, H.; Guo, Z.; Yin, Q.; Wu, H.; Xu, C.; Zhang, E.; Shi, J.; Cheng, J.; Xiao, X.; et al. The position of the Current Warm Period in the context of the past 22,000 years of summer climate in China. *Geophys. Res. Lett.* **2021**, *48*, e2020GL091940. [[CrossRef](#)]
50. Marcott, S.; Shakun, J.; Clark, P.U.; Mix, A. A reconstruction of regional and global temperature for the past 11,300 years. *Science* **2013**, *339*, 1198–1201. [[CrossRef](#)]
51. Liu, W.G.; Huang, Y.; An, Z.; Clemens, S.C.; Li, L.; Prell, W.L.; Ning, Y. Summer monsoon intensity controls C4/C3 plant abundance during the last 35 ka in the Chinese Loess Plateau: Carbon isotope evidence from bulk organic matter and individual leaf waxes. *Palaeogeogr. Palaeoclimatol. Palaeoecol.* **2005**, *220*, 243–254. [[CrossRef](#)]
52. Berger, A.; Loutre, M.F.; Yin, Q. Total irradiation during any time interval of the year using elliptic integrals. *Quat. Sci. Rev.* **2010**, *29*, 1968–1982. [[CrossRef](#)]
53. Lu, H.; Zhao, C.; Mason, J.; Yi, S.; Zhao, H.; Zhou, Y.; Ji, J.; Swinehart, J.; Wang, C. Holocene climatic changes revealed by aeolian deposits from the Qinghai Lake area (northeastern Qinghai-Tibetan Plateau) and possible forcing mechanisms. *Holocene* **2011**, *21*, 297–304.
54. Lu, R.; Jia, F.; Gao, S.; Shang, Y.; Li, J.; Zhao, C. Holocene aeolian activity and climatic change in Qinghai Lake basin, northeastern Qinghai-Tibetan Plateau. *Palaeogeogr. Palaeoclimatol. Palaeoecol.* **2015**, *430*, 1–10. [[CrossRef](#)]
55. Shaowu, W. Abrupt climate change and collapse of ancient civilizations at 2200BC–2000BC. *Prog. Nat. Sci.* **2005**, *15*, 908–914. [[CrossRef](#)]

Disclaimer/Publisher’s Note: The statements, opinions and data contained in all publications are solely those of the individual author(s) and contributor(s) and not of MDPI and/or the editor(s). MDPI and/or the editor(s) disclaim responsibility for any injury to people or property resulting from any ideas, methods, instructions or products referred to in the content.